232

A Study on an Autonomous Operation System of Caisson Shovels in High Air Pressure and Narrow Underground Space
(Development of a 1/10-scale Test Platform and its Demonstration)

Toshitaka TSUNEKI[*1], Naoto NEGISHI[*1], Ryota TSUCHIYA[*1], Koki KIKUCHI[*1], Toshihiro KONDO[*2], Tetsuya KOYO[*2], Akira KAMEI[*2] and Keigo HAYAKAWA[*2]

*1 The Department of Advance Robotics, Chiba Institute of Technology
2-17-1 Tsudanuma, Narashino, Chiba 275-0016, JAPAN
s1326084yu@s.chibakoudai.jp, s1226082wt@s.chibakoudai.jp,
s1426083qd@s.chibakoudai.jp, kikut@ieee.or.jp

*2 Oriental Shiraishi Corp.
5-6-52 Toyosu, Koto-ku, Tokyo 135-0061, JAPAN
toshihiro.kondo@orsc.co.jp, tetsuya.koyou@orsc.co.jp,
akira.kamei@orsc.co.jp, keigo.hayakawa@orsc.co.jp

Abstract
In this study, we aim to achieve unmanned construction for a pneumatic caisson method operating in high air pressure and narrow space and develop a 1/10-scale test platform for an autonomous system of caisson shovels. This platform consists of the caisson box with a working chamber mounted on rail tracks on the ceiling and shafts for passing through the earth bucket, etc., caisson shovels with five degrees of freedom, and ground made of soil, which are scaled down and fabricated. Using this test platform, two types of human-operated excavation method, on-board operation and teleoperation, are verified and the effective operation method is investigated. First, the trajectories obtained by on-board operation and teleoperation were analyzed through image processing and the excavation performance was shown. For excavation by teleoperation, the motion in the direction of the line of sight of the camera deteriorated because of the lack of a three dimensional perspective view. Next, the excavation motions by on-board operation and teleoperation were reproduced by the fabricated 1/10-scale test platform and the reproducibility was investigated. The result revealed that both trajectories corresponded qualitatively and the errors normalized by the bucket length were 4.8% for the bucket joint and 8.3% for the bucket claw in case of on-board operation and 5.0% for the bucket joint and 7.9% for the bucket claw in case of teleoperation, respectively. Moreover, manipulability and manipulating force ellipsoids that were nearly perfect circles revealed that the caisson shovel could move the bucket and exert force in any direction on the sagittal plane.

Keywords: unmanned construction, pneumatic caisson method, excavation, 1/10-scale test platform, shovel

1 Introduction
Construction works such as bridge structures, vertical shafts for subways and tunnels, sewer plants, and underground water reservoirs require the excavation of a deep and large underground space. A pneumatic caisson method (PCM) [1], [2], which is a typical excavation method, immerses a reinforced concrete caisson box vertically by excavating the earth using teleoperated shovels mounted on a rail track on the ceiling of a sealed working chamber, in which high air pressure is maintained in order to avoid groundwater invasion, as shown in **Fig.1**. This construction method achieves deep and large construction to a depth of 73.1m for a 32.6m*42.1m site or a depth of 43.7m for a 62.1m*77.9m site, does not block natural groundwater veins, and allows construction even on water. However, there are some disadvantages. For example, in the case of teleoperation, the view of the camera mounted on the shovel is limited, which decreases the excavation efficiency. Moreover, a large number of shovels for large scale construction require the same number of human operators. The maintenance, assembly, and disassembly in the high air pressure working chamber may cause health hazards.

For these reasons, unmanned construction technology has been studied and a number of robots have been proposed and developed. Hitachi Construction Machinery Co., Ltd. [3] and Hitachi Power Solutions Co., Ltd. [4] have sent the unmanned construction technology to the market. For example, Advance System with Twin Arm for Complex Operation (ASTACO-SoRa) [5], which is a teleoperated twin arm robot having dimensions of 98cm*157cm*150cm (2.5ton), is driven by a diesel engine and is teleoperated by six cameras. The potential of the ASRACO-SoRa was demonstrated when this robot was used to remove rubbles at FUKUSHIMA DAIICHI nuclear power plant. Kang *et al*. [6] proposed a three dimensional path tracking strategy for an engine-driven 21ton class hydraulic excavator with a 2.92m arm. Although they achieved good on-site performance, we cannot use these systems in our caisson facility because (1) the machine must pass through a narrow material shaft having a diameter of 1.08m and (2) the combustion engine cannot be used in the sealed high air pressure working chamber.

From these points of view, we propose a PCM for unmanned construction under high air pressure in a

narrow space. In this study, we develop a 1/10-scale test platform for an autonomous operation system of caisson shovels. This test platform consists of a caisson box with a working chamber mounting rail tracks on the ceiling and material shafts for the installation of the earth bucket, etc., caisson shovels with five degrees of freedom (DOFs), and ground made of sandy soil, all of which are scaled down and fabricated. Using this test platform, two types of human-operated excavation method, namely, on-board operation and teleoperation, are demonstrated and verified.

The remainder of this paper is organized as follows. In Section 2, we describe the architecture of the 1/10-scale test platform. In Section 3, we describe the mathematical model of the caisson shovel and define the manipulability and manipulating force. In Section 4, we experimentally investigate the motion trajectories of on-board operation and teleoperation. In Section 5, we reproduce the motion by the 1/10-scale test platform and discuss the motion characteristics. Finally, in Section 6, we conclude the paper and outline future research.

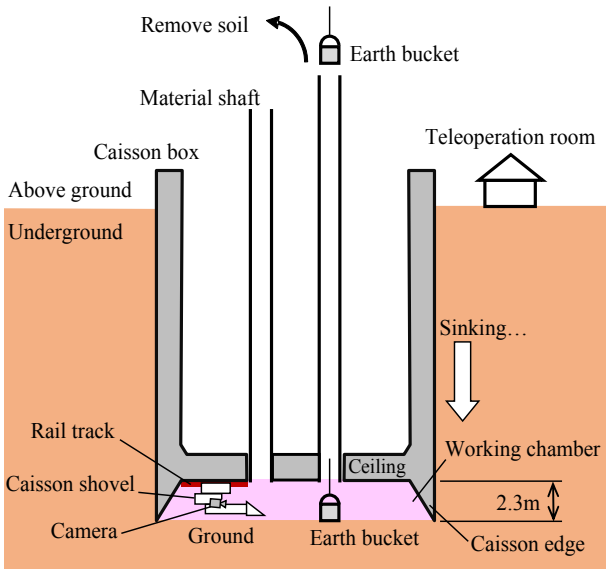

Fig. 1 Pneumatic caisson facilities

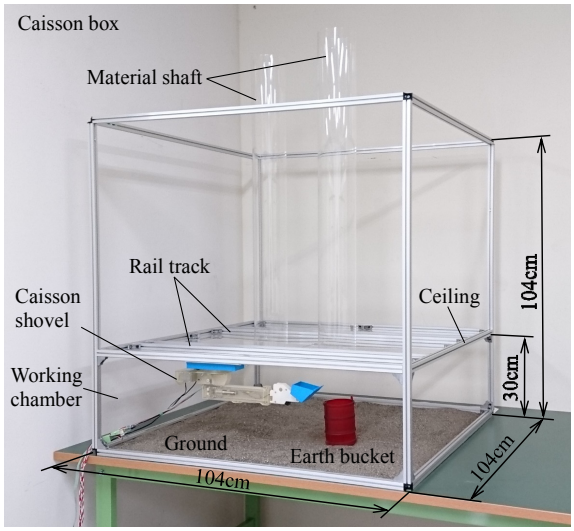

Fig. 2 Fabricated 1/10-scale test platform

2 1/10-scale test platform

The 1/10-scale test platform consists of a caisson box with a working chamber, an earth bucket, a caisson shovel, and ground made of sandy soil. **Figure 2** shows the fabricated platform.

2.1 Caisson box and earth bucket

The caisson box with dimensions of 104cm*104cm*104cm was constructed of aluminum and has a 30cm-high working chamber at its bottom. Although the practical height keeps 230cm, this model has the margin for the soil thickness of 7cm. The ceiling of the working chamber has two pairs of rail tracks on which the shovel can travel and two material shaft holes with an internal diameter of 10.8cm, through which, e.g., the earth bucket and disassembled shovel parts are passed. Note that, in order to focus on the shovel operation, the high air pressure environment in the working chamber is not reproduced in this study. The earth bucket, which has a diameter of 10.3cm and a height of 13.5cm, is passed through the material shaft hole by a wire cable and transfers the soil loaded by the shovel to the surface ("Above ground" in **Fig.1**).

2.2 Caisson shovel

Figure 3 shows the fabricated 1/10-scale caisson shovel, which is mounted on a rail track on the ceiling. The reaction force generated by the caisson shovel is countered by the ceiling and the caisson shovel stably exerts a larger bucket force, as compared to the common backhoe [7], which is supported by the unstable rough ground. The caisson shovel consists of four parts: carriage, boom, counter weight, and bucket units, which are inserted through the material shaft and assembled in the working chamber. After construction is complete, these are disassembled and removed through the material shaft. The shovel has five DOFs: travel along the rail track (d_0), yaw rotation of the boom unit (θ_1), pitch rotation (dumping) of the boom unit (θ_2), expansion and contraction of the boom unit (d_3), and pitch rotation of the bucket unit (θ_4). The expansion and contraction of the boom unit are driven by a DC motor with a gear and an encoder (maxon motor, 10.4W, 326:1, 128P/R) and controlled by PWM signals from a microcomputer (mbed, NXP LPC 1768). The others are driven by servo motors (KONDO KAGAKU CO., LTD., KRS-4034HV ICS, KRS-2542 ICS). The sampling time is 20ms for a feedback control. The mbed is also used as a CPU. Note that the practical caisson shovel is driven by hydraulic cylinders using the electric power supply.

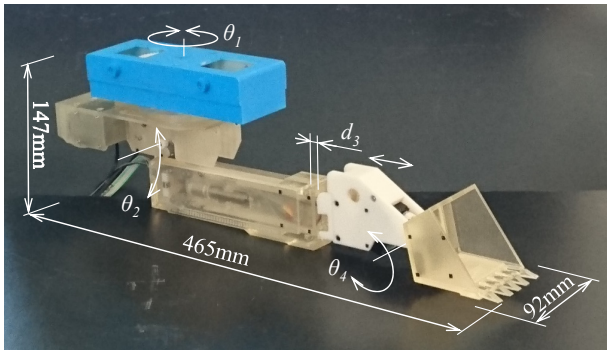

Fig. 3 Fabricated 1/10-scale caisson shovel

2.3 Ground of sandy soil

The actual ground below the working chamber is rough terrain, as shown in **Fig. 4**, and the soil property depends strongly on the construction site. Here, we focus on not the soil properties, such as viscosity and permeability, but rather the three dimensional rise-and-fall and reproduce the ground using sand. Note that this 3D geometric information is recognized by a depth sensor (Kinect v2) mounted on the caisson shovel.

Fig. 4 Example of the practical ground condition below the working chamber

3 Caisson shovel model

3.1 Mathematical model and kinematics

Figure 5 shows the mathematical link model of the caisson shovel and the coordinate systems. This is the initial configuration when $d_0 = \theta_1 = \theta_2 = d_3 = \theta_4 = 0$. Here, Σ_R is the frame of reference and Σ_E is the coordinate system of the bucket claw. **Table 1** shows the link parameters [8] from Σ_1 to Σ_E. From the link parameters and the relationship between Σ_R and Σ_0, the homogeneous transformation matrix is obtained as

$$ {}^{R}T_{H} = \begin{bmatrix} C_1C_{2+4} & -S_1 & -C_1S_{2+4} & p_x \\ S_1C_{2+4} & C_1 & -S_1S_{2+4} & p_y \\ S_{2+4} & 0 & C_{2+4} & p_z \\ 0 & 0 & 0 & 1 \end{bmatrix} $$

where

$$ \begin{aligned} p_x &= C_1(l_6S_{2+4} + l_5C_{2+4} - l_3C_2 + (d_3 + l_4)S_2 - l_2) + d_0 \\ p_y &= S_1(l_6S_{2+4} + l_5C_{2+4} - l_3C_2 + (d_3 + l_4)S_2 - l_2) \\ p_z &= -l_6C_{2+4} + l_5S_{2+4} - l_3S_2 - (d_3 + l_4)C_2 - l_1 \end{aligned} \quad (1) $$

Here, $S_i \equiv \sin\theta_i$ and $C_i \equiv \cos\theta_i$. Then, the relationship between the position and orientation of the bucket claw, ***r***, is

$$ \boldsymbol{r} = \begin{bmatrix} x_E \\ y_E \\ z_E \\ \Phi \\ \Theta \\ \Psi \end{bmatrix} = \begin{bmatrix} p_x \\ p_y \\ p_z \\ \theta_1 \\ \theta_2 + \theta_4 \\ 0 \end{bmatrix} \quad (2) $$

where Φ, Θ, and Ψ are the yaw, pitch, and roll angles, respectively. Hence, this mechanism cannot change the roll angle. Except for the role angle, the position and orientation are uniquely determined by five DOF variables. Note that the link lengths are as follows: l_1 is 829mm, l_2 is 170mm, l_3 is 415mm, l_4 is 2631mm, l_5 is 813mm, and l_6 is 259mm.

Next, assuming that d_0=0 under the excavation, we obtain the inverse kinematics of the caisson shovel, because the carriage unit is fixed on the rail track in order to support the reaction force stably during excavation operation. From inverse kinematics, the position and pitch angle of the bucket claw is obtained as

$$ \begin{bmatrix} \theta_1 \\ \theta_2 \\ d_3 \\ \theta_4 \end{bmatrix} = \begin{bmatrix} \arctan_2(y_E, x_E) \\ \arctan_2(k_1, k_2) - \arctan_2(\sqrt{k_1^2 + k_2^2 - l_3^2}, l_3) \\ (x_E / C_1 - l_6S_\Theta - l_5C_\Theta + l_3C_2 + l_2)/S_2 - l_4 \\ \Theta - \theta_2 \end{bmatrix} \quad (3) $$

where

$$ \begin{aligned} k_1 &= -l_6C_\Theta + l_5S_\Theta - l_1 - z_E \\ k_2 &= -l_6S_\Theta + l_5C_\Theta - l_2 - y_E / S_1 \end{aligned} $$

The velocity and angular velocity of the bucket claw are given by

$$ \begin{bmatrix} \dot{x}_E \\ \dot{y}_E \\ \dot{z}_E \\ \dot{\Phi} \\ \dot{\Theta} \\ \dot{\Psi} \end{bmatrix} = J \begin{bmatrix} \dot{d}_0 \\ \dot{\theta}_1 \\ \dot{\theta}_2 \\ \dot{d}_3 \\ \dot{\theta}_4 \end{bmatrix} = \begin{bmatrix} 1 & J_{12} & J_{13} & J_{14} & J_{15} \\ 0 & J_{22} & J_{23} & J_{24} & J_{25} \\ 0 & J_{32} & J_{33} & J_{34} & J_{35} \\ 0 & 1 & 0 & 0 & 0 \\ 0 & 0 & 1 & 0 & 1 \\ 0 & 0 & 0 & 0 & 0 \end{bmatrix} \begin{bmatrix} \dot{d}_0 \\ \dot{\theta}_1 \\ \dot{\theta}_2 \\ \dot{d}_3 \\ \dot{\theta}_4 \end{bmatrix} $$

where

$$ \begin{aligned} J_{12} &= -S_1(l_6S_{2+4} + l_5C_{2+4} - l_3C_2 + (d_3 + l_4)S_2 - l_2) \\ J_{13} &= C_1(l_6C_{2+4} - l_5S_{2+4} + l_3S_2 + (d_3 + l_4)C_2) \\ J_{14} &= S_2, \quad J_{15} = C_1(l_6C_{2+4} - l_5S_{2+4}) \\ J_{22} &= C_1(l_6S_{2+4} + l_5C_{2+4} - l_3C_2 + (d_3 + l_4)S_2 - l_2) \\ J_{23} &= S_1(l_6C_{2+4} - l_5S_{2+4} + l_3S_2 + d_3C_2 + l_4C_2) \\ J_{24} &= S_2, \quad J_{25} = S_1(l_6C_{2+4} - l_5S_{2+4}) \\ J_{32} &= 0 \\ J_{33} &= l_6S_{2+4} + l_5C_{2+4} - l_3C_2 + d_3S_2 + l_4S_2 \\ J_{34} &= -C_2, \quad J_{35} = l_6S_{2+4} + l_5C_{2+4} \end{aligned} \quad (4) $$

and J is a Jacobian matrix. The caisson shovel is in a singular configuration, when $\det(J^T J) = 0$. In this study, since the carriage unit is fixed ($\dot{d}_0 = 0$) during the excavation and the roll angle is not controlled (Ψ=0), the Jacobian matrix becomes

$$ J_{55} = \begin{bmatrix} J_{12} & J_{13} & J_{14} & J_{15} \\ J_{22} & J_{23} & J_{24} & J_{25} \\ J_{32} & J_{33} & J_{34} & J_{35} \\ 1 & 0 & 0 & 0 \\ 0 & 1 & 0 & 1 \end{bmatrix}. \quad (5) $$

The inverse problem is solved by J_{55}^{-1}. In this study, based on the geometric condition, the caisson shovel is operated around $\theta_1 = 0$ and $\theta_2 = 90°$. In addition, the 1/10-scale caisson shovel cannot reproduce the dynamics of the actual caisson shovel because the inertia differs by 10^{-5} and the weight differs by 10^{-3} due to the scale effect. Based on these equations, the 1/10-scale caisson shovel is controlled by PWM signals with a sampling time of 1ms.

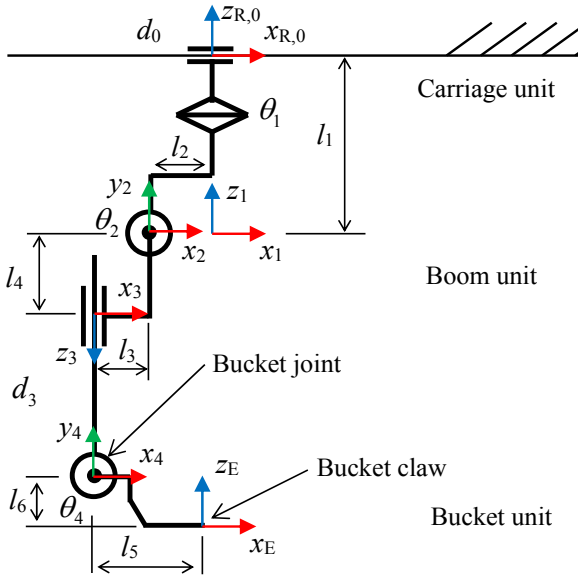

Fig. 5 Mathematical link model of the caisson shovel

Table 1 Link parameters

i	a_{i-1}	α_{i-1}	d_i	θ_i
1	0	0	$-l_1$	θ_1
2	$-l_2$	90°	0	θ_2
3	$-l_3$	90°	d_3+l_4	0
4	0	-90°	0	θ_4
E	l_5	-90°	$-l_6$	0

3.2 Manipulability and manipulating force

In this study, the manipulability is defined as the volume of the set of velocity vectors of the bucket joint under the condition in which the carriage unit is fixed and the sum of the squared normalized driving angular and translational velocities is less than 1.0, i.e.,

$$\dot{d}_0 = 0$$
$$\left(\frac{\dot{\theta}_1}{\max\dot{\theta}_1}\right)^2 + \left(\frac{\dot{\theta}_2}{\max\dot{\theta}_2}\right)^2 + \left(\frac{\dot{d}_3}{\max\dot{d}_3}\right)^2 \le 1 \qquad (6)$$

where the denominators are the maximum angular and translational velocities of the actual bucket joint, i.e., $\max\dot{\theta}_1$=0.4 [rad/s], $\max\dot{\theta}_2$=0.05 [rad/s], and $\max\dot{d}_3$ =0.17 [m/s]. Thus, the set of the velocity vectors of the bucket joint becomes an ellipsoid and the volume is then proportional to the absolute determinant of the normalized Jacobian matrix J_n.

$$J_n = \begin{bmatrix} J_{12} & J_{13} & J_{14} \\ J_{22} & J_{23} & J_{24} \\ J_{32} & J_{33} & J_{34} \end{bmatrix} \begin{bmatrix} \max\dot{\theta}_1 & 0 & 0 \\ 0 & \max\dot{\theta}_2 & 0 \\ 0 & 0 & \max\dot{d}_3 \end{bmatrix}^{-1}. \qquad (7)$$

Thus, the manipulability is expressed by

$$\omega = \det(J_n^T J_n). \qquad (8)$$

Larger values indicate that the caisson shovel can be agilely moved in any direction. In contrast, a zero indicates that the caisson shovel is in the state of a singular configuration and the velocity cannot be controlled.

On the other hand, the manipulating force is also defined as the volume of the set of force vectors on the bucket joint and is expressed as $1/\omega$. The major axes of the ellipsoid for the manipulating force correspond to those of the manipulability and the lengths are mutually inversely proportional. This means that the direction in which the large force exerts cannot be moved quickly and vice versa, because the manipulability and the manipulating force are in a trade-off relationship. **Figure 6** shows the manipulability ellipsoids (yellow) and manipulating force ellipsoids (light green) when $d_0 = 0$, $\theta_1 = 0$, $\theta_2 = 90°$, $d_3 = 0$, and $\theta_4 = -90°$. The red, green, and blue lines indicate the major axes.

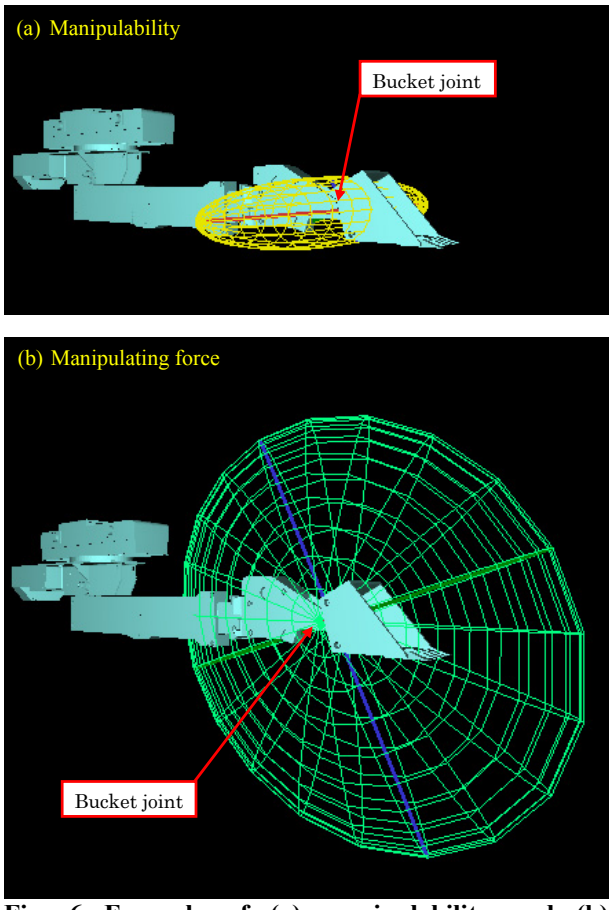

Fig. 6 Example of (a) manipulability and (b) manipulating force ellipsoids

4 On-board operation and teleoperation

In order to investigate the excavation efficiency and the motion characteristics, we experimentally performed two types of excavation method: on-board operation and teleoperation. In on-board operation (**Fig. 7**(a)), the caisson shovel is controlled directly by an operator in the working chamber to excavate the earth. In teleoperation (**Fig. 7**(b)), the caisson shovel is controlled remotely from teleoperation room on 2D camera images sent to operator.

Figure 8 shows the trajectories of the bucket claw (red) and the bucket joint (blue) by (a) on-board operation and (b) teleoperation, the representative manipulability ellipsoids of the bucket joint (yellow), and the representative manipulating force ellipsoids (light green). We found that the stroke of the boom in on-board operation was 30.5% longer than that in teleoperation. This is because, in excavation by teleoperation, the motion in the direction of the line of sight of the camera was hindered due to the lack of 3D perspective view. Hence, this deteriorates the excavation efficiency. Meanwhile, during excavation when the shovel is in contact with the ground, since both the manipulability and the manipulating force were close to a perfect circle, the caisson shovel can move the bucket and exert force in any direction on the sagittal (x-z) plane.

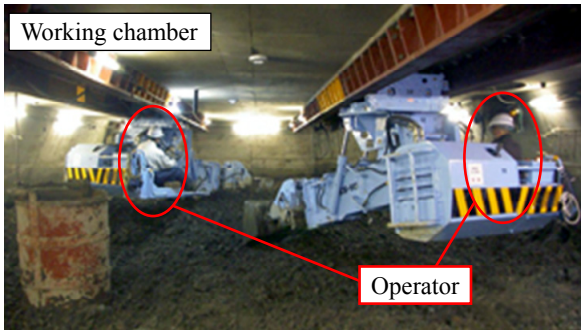

(a) On-board operation

(b) Teleoperation

Fig. 7 Two types of excavation method: (a) On-board operation and (b) teleoperation

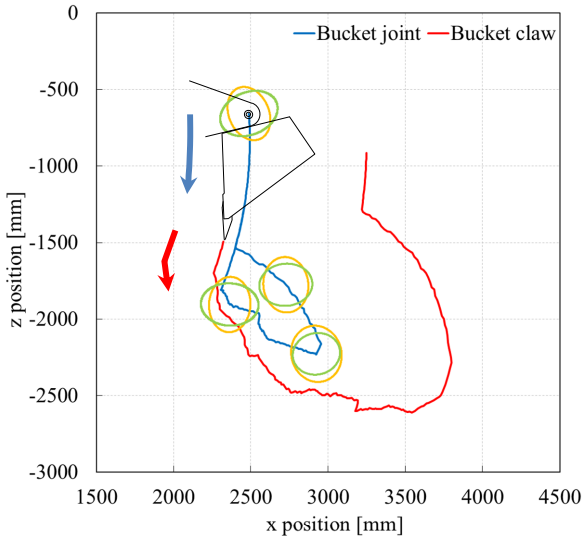

(a) On-board operation

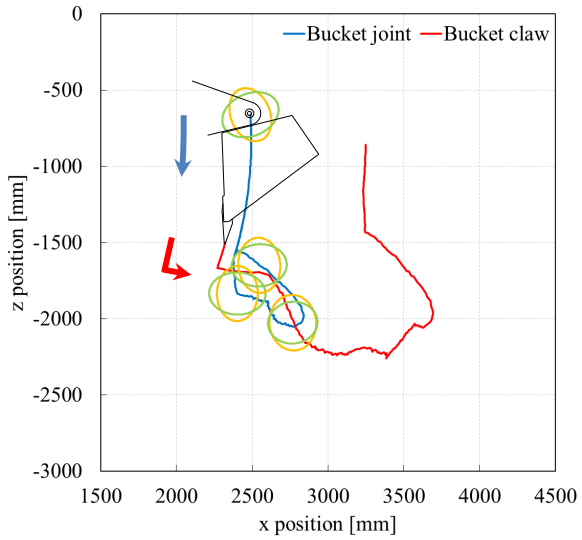

(b) Teleoperation

Fig. 8 Trajectories of the actual caisson shovel by on-board operation and teleoperation

5 Reproducibility by 1/10-scale model platform

In this section, we discuss the reproducibility of the motion of the fabricated 1/10-scale caisson shovel. Although automated excavation by autonomous caisson shovels is important for unmanned construction and experimentation using an actual caisson shovel at an actual construction site is needed, it is difficult in terms of time and cost. Therefore, planning and experimentation using the 1/10-scale test platform is useful and important as a pilot study. Here, we reproduce the excavation motion trajectories for on-board operation and teleoperation and investigate the motion characteristics and accuracy of these trajectories by comparing the reproducibility.

Figure 9 shows the trajectories ((a) on-board operation and (b) teleoperation) reproduced by the 1/10-scale bucket claw (red: Σ_E) and the bucket joint (blue: Σ_4) using a position control, the manipulability ellipsoids of the bucket joint (yellow), and the manipulating force

ellipsoids (green). The trajectories obtained by the 1/10-scale caisson shovel corresponded qualitatively with those of an actual caisson shovel. To compare the errors between the practical and 1/10-scale caisson shovels, we normalized and nondimensionalized them using the characteristic length, i.e., the bucket length. From this, the normalized errors were 4.8% for the bucket joint and 8.3% for the bucket claw in case of on-board operation and 5.0% for the bucket joint and 7.9% for the bucket claw in case of teleoperation, respectively. This is because the sampling time for control was coarse (20ms). Since the inertia and mass of the 1/10-scale caisson shovel are very small (10^{-3} and 10^{-5}) and it is easy to accelerate, the sampling time should be improved. Although the kinematics between the actual caisson shovel and 1/10-scale caisson shovel are approximately the same, the dynamics must be considered from another point of view.

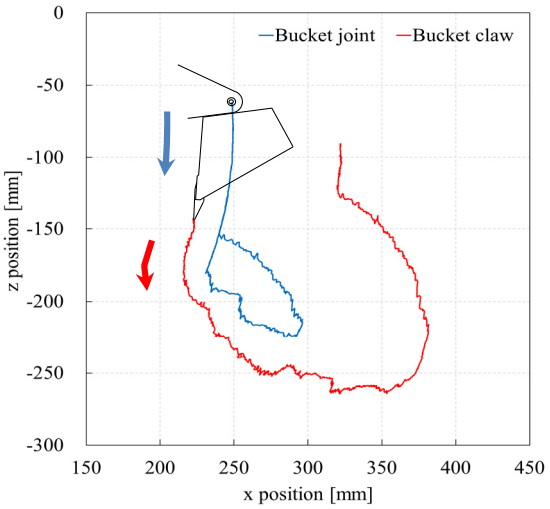

(a) On-board operation

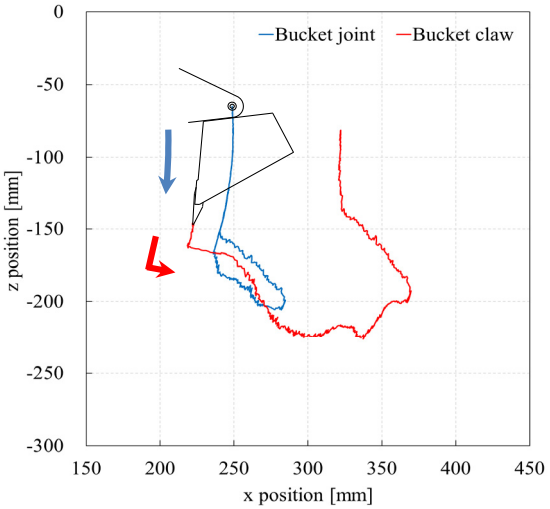

(b) Teleoperation

Fig. 9 Trajectories reproduced by the 1/10-scale caisson shovel for (a) on-board operation and (b) teleoperation

6 Conclusions

In this study, we aim to achieve unmanned construction using a pneumatic caisson method operating in high air pressure and narrow space and developed a 1/10-scale test platform for an autonomous system of caisson shovels. Using this test platform, two types of human operated excavation methods, on-board operation and teleoperation, were verified and the effective operation method was investigated. In excavation by on board operation, the 30% longer stroke motion operation was clarified and in excavation by teleoperation, the motion in the direction of the line of sight of the camera was hindered due to the lack of 3D perspective view. The excavation motions reproduced by the 1/10-scale test platform showed good trajectory tracking performance.

In the future, we intend to demonstrate automatic excavation planning and autonomous excavation by the planned motion trajectory using the 1/10-scale test platform.

Acknowledgements

This research was supported by a grant from the "Sentan Sangyo Souzou Project (Saitama Prefecture)" and by Sankeikogyo Corp. The authors would like to express their deep gratitude to all involved in the research project.

References

[1] http://www.orsc.co.jp/english/tec/newm_v2/ncon02.html.

[2] Kodaki, K., Nakano, M., and Maeda, S., "Development of the automatic system for pneumatic caisson", Automation in Construction, Vol.6, (1997), pp.241-255.

[3] https://www.hitachicm.com/global/ourbusiness/products/double-front-work-machine/

[4] http://www.hitachi-power-solutions.com/

[5] Egawa, E., Dual-arm heavy machinery-type robot "ASTACO-SoRa", Journal of the Japan Society of Mechanical Engineers, Vol.117, No.1151 (2014), pp.682-683 (in Japanese).

[6] Kang, S., Park, J., Kim, S., Lee, B., Kim, Y., Kim, P., and Kim, H., "Path Tracking for Hydraulic Excavator Utilizing Proportional-derivative and Linear Quadratic Control", IEEE Conf. on Control Application, (2014), pp.808-813.

[7] Yamamoto, H., Uesaka, K., Ishimatsu, Y., Yamaguchi, T., Aritomi, K., and Tanaka, Y., "Introduction to the General Technology Development Project: Research and Development of Advanced Execution Technology by Remote Control Robot and Information Technology", ISARC, 2006.

[8] Denavit J. and Hartenberg, R.S., "A Kinematic Notation for Lower-Pair Mechanisms Based on Matrices", ASME Journal of Applied Mechanics, Vol. 77, (1955), pp.215-221.

Received on December 29, 2016
Accepted on March 29, 2017